VIP Mesoporous Materials Very Important Paper

Deutsche Ausgabe: DOI: 10.1002/ange.201500659
Internationale Ausgabe: DOI: 10.1002/anie.201500659

Interrupted Chalcogenide-Based Zeolite-Analogue Semiconductor: Atomically Precise Doping for Tunable Electro-/Photoelectrochemical Properties**

Jian Lin, Youzhen Dong, Qian Zhang, Dandan Hu, Na Li, Le Wang, Yang Liu,* and Tao Wu**

Abstract: *Incorporation of semiconductor property into zeolite materials is a plausible approach to graft oxide zeolites with multifunctionality in which both electronic/optoelectronic functions and high porosity are integrated. However, creating such semiconductor zeolites, especially the ones with controllable function regulation still remains as a great synthetic challenge over the years. Hereby, we reported the first case of an interrupted chalcogenide-based zeolite-analog semiconductor with an entirely new boracite-related framework and specific sites at the interrupted section. The semiconducting nature and band structure of this open-framework n-type semiconductor material were characterized with solid-state UV/Vis diffuse reflectance spectroscopy and Mott–Schottky measurements. More importantly, the In–Se chalcogenide zeolite analog was for the first time explored as an effective electrocatalyst for the oxygen reduction reaction (ORR). The specific indium sites served as active centers and proved to be responsible for a superior ORR activity. Meanwhile, these specific sites could be precisely replaced by bismuth(III) ions, leading to facile manipulation in their electro-/photoelectrochemical properties. Such atomically precise doping successfully implemented at the semiconductor zeolite material with specifically interrupted sites presents a very promising route for accurately regulating electronic structure and photoelectrical properties of other open-framework semiconductor materials.*

Zeolites, as an important class of inorganic crystalline microporous materials, are widely used in petroleum refining and fine chemical industry as catalysts.[1] Enormous economic benefits brought by these porous materials have stimulated long-lasting academic research interest in exploration of zeolite materials with variable composition and new types of frameworks. Therefore, the number of zeolite framework type codes assigned by the Structure Commission of the International Zeolite Association (SC-IZA) has experienced a rapid growth in recent years,[2] especially when new structure determination techniques (such as electron crystallography and model-building) are used for ultra-small single crystals.[3] However, the inherent insulating characteristic of oxide-based zeolites greatly limits their applications in the aspect of photo-/electric-related processes. To solve this problem, great efforts have been devoted to creating chalcogenide-based semiconductor zeolites (CSZ) by simultaneously replacing oxygen with chalcogen (S/Se/Te) and Si/Al with tetrahedrally coordinated main-group metal ions (such as In/Ga/Sn/Ge).[4] Such methodology is proved to have successfully integrated both zeolitic architecture and semiconductor properties into one material which possesses both high specific surface area and UV/Vis photocatalytic activity. However, to our best knowledge, there is only one out of 225 zeolite framework types in newly released zeolite database, which is composed by metal chalcogenide (coded as RWY).[2,4] In fact, three other metal chalcogenides with zeolitic framework reported in Ref. [4] were not coded by SC-IZA. Because the variable connecting modes (μ_2-, μ_3- and μ_4-) adopted by the chalcogen anions inevitably leads to more complicated non-zeolitic structures, especially under the absence of the tetravalent metal ions in the system.[5] Synthesizing CSZs with more diverse composition and achieving visible-light activity is of great importance, however, still very challenging.

Other than the concern on the composition of zeolite materials, on a structural aspect, there is always great interest in searching for the zeolites with large or extra-large pores.[6] Interrupted sites (i.e. tetrahedrally coordinated cations are bonded to one or two terminal hydroxides), as a naturally occurring phenomenon in oxide-based zeolite framework formation, is generally accepted to facilitate the construction of extra-large pores or channels. Among the reported oxide-based zeolites, 11 out of 224 frameworks have been found to possess interrupted sites.[2] More recently, in metal–organic framework zeolite analogs, interrupted sites have also been found in ZIF-100[7] with a colossal cage and BIF-201.[8] However, these earlier researches on interrupted zeolitic

[*] J. Lin,[+] Q. Zhang, D. D. Hu, Prof. Dr. N. Li, Dr. L. Wang, Prof. Dr. T. Wu
The Key Lab of Health Chemistry and Molecular Diagnosis of Suzhou, College of Chemistry Chemical Engineering and Materials Science
Soochow University, Suzhou Jiangsu 215123 (China)
E-mail: lewang@suda.edu.cn
wutao@suda.edu.cn

Y. Z. Dong,[+] Prof. Dr. Y. Liu
Key Lab of Bioorganic Phosphorus Chemistry and Chemical Biology, Department of Chemistry
Tsinghua University, Beijing 100084 (China)
E-mail: liu-yang@mail.tsinghua.edu.cn

[+] These authors contributed equally to this work.

[**] This work was supported by the National Natural Science Foundation of China (grant numbers 21271135 and 21375073), a start-up fund from Soochow University (grant number Q410900712), the Priority Academic Program Development of Jiangsu Higher Education Institutions (PAPD), and the Young Thousand Talented Program. T.W. thanks Prof. Michael O'Keeffe and Dr. Charlotte Bonneau for topological analysis.

Supporting information for this article is available on the WWW under http://dx.doi.org/10.1002/anie.201500659.

structures have mainly focused on the structural features or the introduction of specific sites as catalytically active sites, seldom if any, studied the possibility of specific site modification towards function regulation. In CSZ materials, ordered interrupted sites are highly desirable because they cannot only serve as unique active sites for selectively catalytic reactions but also allow for atomically precise doping for purposely tuning of the electric or photoelectric properties.

Herein, we reported an interrupted chalcogenide-based zeolite-analog semiconductor $([In_{28}Se_{54}(H_2O)_4]^{24-}\cdot 24(H^+\text{-PR})\cdot n H_2O$, denoted as **CSZ-5-InSe**, H^+-PR = protonated piperidine). It features an entirely new boracite-related topology and specific sites at the interrupted section. These interrupted indium sites embedded in the open-framework n-type semiconductor zeolite material are proved to be active centers, answering for good performance on electrocatalytic oxygen reduction reaction. Interestingly, these specific sites are available for atomically precise doping exemplified by Bi^{III} ions, giving rise to fine-tuning of the electro-/photoelectrochemical properties.

Dark red cubic crystals of **CSZ-5-InSe** were synthesized by solvothermal reaction of elemental indium and selenium powders in the mixture solvents of piperidine (PR) and deionized water at 170 °C for 7 days. The structure and composition of **CSZ-5-InSe** were characterized by single-crystal X-ray diffraction (SCXRD), temperature-programmed desorption mass spectroscopy (TMP-MS), elemental analysis (EA), and its solid-state stability as well as phase purity were identified by powder XRD (PXRD) and thermal gravimetric analysis (TGA), respectively (see Tables S1,S2, Figures S1–S3 in the Supporting Information). The single-crystal structure refinement shows that **CSZ-5-InSe**, crystallizing in the cubic space group $F\bar{4}3c$, contains three independent indium ions in an asymmetrical unit (Figure S4): both In1 and In2 are connected to four In^{3+} ions through μ_2-Se^{2-}, and In3 only connected to three In^{3+} ions through μ_2-Se^{2-} and interrupted by a neutral terminal water molecule at the fourth direction. The completely tetrahedral coordination mode of In^{3+} ions together with the bi-coordinated mode of Se^{2-} ions endows **CSZ-5-InSe** with a typically zeolitic framework (Figure 1 a).

In the zeolitic framework of **CSZ-5-InSe**, a three-membered ring (3-MR) serves as primary building unit, which is preferred in the CSZ system as a result of smaller bond strain derived from a longer bond length of M-S/Se than that of Si/Al-O.[4] Four 3-MRs can fuse together to form a 3*1 secondary building unit (SBU). This unique SBU has not yet been observed in an oxide-based zeolitic framework, but only been found in a chalcogenide zeolite analog of UCR-20 with RWY topology.[2,4] To better understand the structure of **CSZ-5-InSe**, we here simplify it as cluster-based framework. The framework of **CSZ-5-InSe** contains two types of secondary building units: supertetrahedron cluster A $[In_4Se_{10}]$ and supertetrahedron cluster B $[In_4Se_9O]$ (Figure 1 b). Cluster A is connected to four clusters B through corner-sharing mode, while cluster B is connected to three clusters A and leaves the fourth corner interrupted by a neutral water molecule, in which the interrupted indium metal site bonded to H_2O is denoted as specific site X (Figure S5). The intercluster connectivity provides two types of cages: cage α consisting of six clusters A and four clusters B is an extended adamantane cage with six 12-MR window apertures (7.58*7.04 Å with consideration of the Van der Waals radius; Figure 1 c); cage β composed of twelve clusters A and sixteen clusters B possesses a large pore with four 12-MR window apertures and six 16-MR window apertures (Figure 1 d). Each cage β is filled with twenty four H^+-PR species, and no H^+-PR species are found within the cage α. In fact, cage β surrounded by eight cages α could be formed through four fused cages α by missing the central shared cluster A (Figure S6), which means there are periodically cluster-based vacant sites in the framework of **CSZ-5-InSe**. It is obviously observed that 16-MR is enclosed to four "cantilevers" from cluster B, two of them directing to the center of cage β and the other two pointing to the outside of the same cage β. Two sets of enclosed "canti-

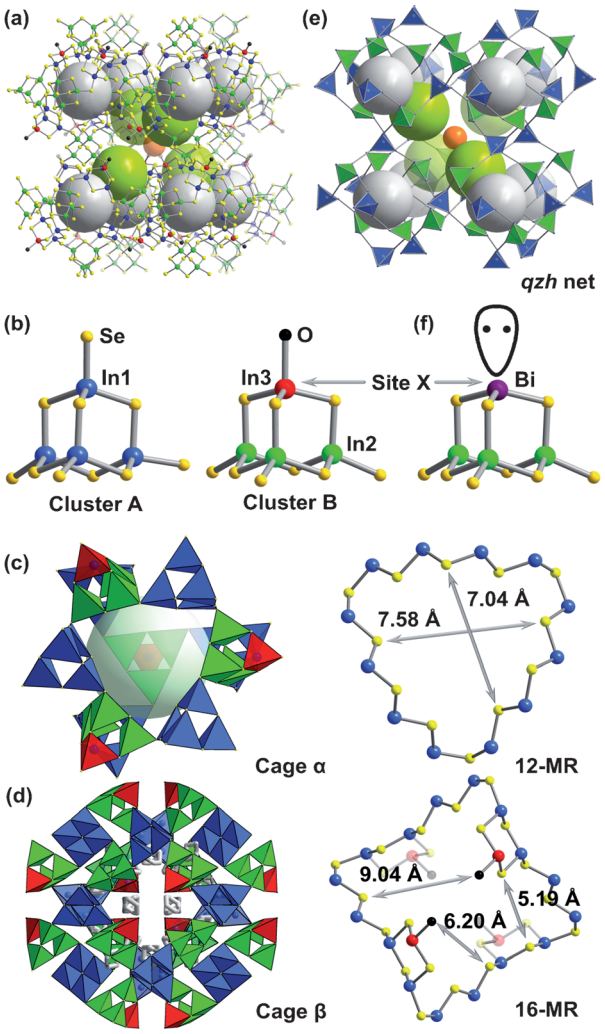

Figure 1. a) 3D zeolitic framework of **CSZ-5-InSe**. b) Supertetrahedron cluster A $[In_4Se_{10}]$ and cluster B $[In_4Se_9O]$. c) Adamantane cage α with 12-MR window aperture. d) Large cage β with 16-MR window aperture and filled with 24 H^+-PR. e) (3,4)-connected ***qzh*** net. f) Bismuth-doped cluster B at specific site X. (green ball: In1; blue ball: In2; red ball: In3; black ball: O from water molecule; yellow ball: Se; large gray sphere: pore in the cage α; large green sphere: pore in cage β; small orange sphere: cluster-based vacancy in center of cage β).

levers" in 16-MR give rise to four lateral-broken 10-MR (9.04*6.20 Å). The connectivity between cage α and cage β also leads to a multiple channel system: channel I with 12-MR aperture along ⟨100⟩ direction and channel II with 16-MR aperture along ⟨110⟩ direction (Figure S7). The unique "cantilever" structure in the cage β reduces the size of channel II, and makes **CSZ-5-InSe** seem like an inorganic "cardiac valve" that may limit the degree of freedom of the molecule diffusion in the framework.

The most prominent structural feature of **CSZ-5-InSe** is its interrupted network exclusively formed by 3-MR. Even though there are only six cases with the framework exclusively formed by 3-MR in the zeolite framework database,[2] no one is associated with an interrupted structure. The occurrence of 3-MR generally leads to a low framework density (FD_T, defined as the number of T atoms in 1000 Å^3), as observed in oxide-based zeolites.[9] Interestingly, integration of the interrupted framework with the exclusive primary building unit 3-MR makes such a net bearing quite low framework density. The FD_T of **CSZ-5-InSe** is 3.87, much lower than that of oxide-based zeolites, and even lower than the previously reported chalcogenide framework (UCR-20) with the lowest FD_T (4.39). Although **CSZ-5-InSe** is bestowed with a zeolitic framework due to tetrahedrally coordinated metal sites, the interrupted structure leads to a previously unknown (3,4)-connected net with vertex symbols (3.12.3.12.3.*)(3.122.3.16.3.16)(3.3.3) (Figure 1e, Table S3). As a matter of fact, it has recently been officially collected into the Reticular Chemistry Structure Resource (RCSR) database and denoted as *qzh*-type net. The *qzh* net is very close to, but different with, the topology of *bor-a*. In addition, while the aforementioned clusters A and B are treated as pseudo-atom, the framework of **CSZ-5-InSe** could be further simplified into well-known (3,4)-connected *bor* topology. The detailed topological differences and their derivative relationship between *bor*/*bor-a* and *qzh* are illustrated in Figure S8 and Table S4.

Another important feature of the interrupted framework of **CSZ-5-InSe** is the atomically precise doping at the specific indium site X. It is well-known in oxide-based zeolites that the type and location of the tetrahedral atoms are associated with variations in bond angles as well as the pore architectures, which may eventually affect their catalytic properties. Likewise, the specific metal site X in **CSZ-5-InSe** inspires us to investigate its feasibility of precise doping for purposefully changing its optical and electrical properties. Considering the distorted tetrahedral chemical environment of the specific indium site which is surrounded by three Se^{2-} anions and one H_2O molecule, Bi is chosen as a perfect candidate in the study of atomically precise doping. Once a Bi source is introduced into the reaction system, it could only be fitted into the interrupted metal site in the form of trivalent Bi^{3+} with pyramidal three-coordinated $BiSe_3$ with a lone pair of electrons since the tetrahedrally coordinated pentavalent Bi^{5+} ion in selenides is extremely unstable (Figure 1f). As designed, bismuth-doped crystals of **CSZ-5-InSe** (denoted as **CSZ-5-InBiSe**) were successfully prepared. The PXRD pattern of **CSZ-5-InBiSe** matches well with its simulated pattern (Figure S1). Although the SCXRD analysis could not fully differentiate Bi from In, the EDS and XPS data beyond doubt prove that the specific sites X are exclusively doped by Bi^{3+} ions, and no Bi^{5+} ions are present at other metal sites. There are 32 interrupted metal sites out of all 224 metal sites in a crystallographic unit cell. EDS analysis shows that the molar percentage content of Bi out of all metal sites is always less than the ideal doping value (32/224 = 14.3%) no matter how much amount of Bi source was added (Figure S9). Bi XPS indicates a 4f multipeak at the binding energy between 157.3 eV ($4f_{7/2}$) and 162.6 eV ($4f_{5/2}$) with a separation of 5.3 eV, which are in good agreement with Bi^{3+}, as observed in Bi_2Se_3 (Figure S10).[10]

Further exploration for potential applications of **CSZ-5** necessitates a detailed characterization of its band structure. Hence, solid-state UV/Vis diffuse reflectance spectroscopy (DRS) and Mott-Schottky (MS) measurements using electrochemical impedance techniques were used to characterize band gap, and the band position of conduction band (CB) and valence band (VB). Optical absorption investigation reveals that **CSZ-5-InSe** and **CSZ-5-InBiSe** have a direct band gap (E_{BG}) of 2.10 and 2.03 eV, respectively, by extrapolating the linear region of the plot of the absorbance square versus the energy from the absorption edge (Figure 2a). These values,

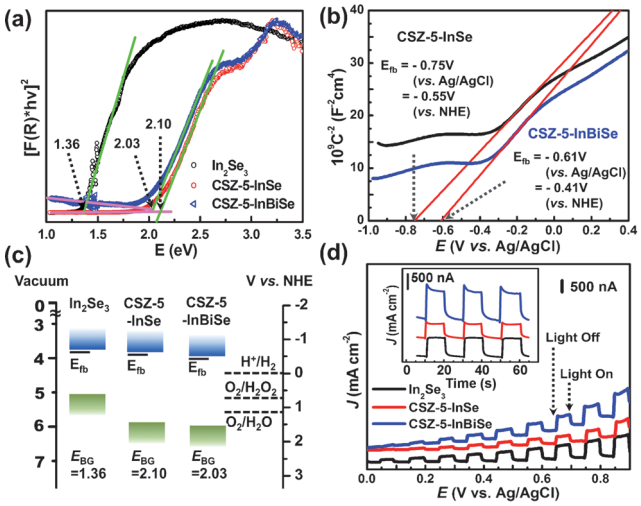

Figure 2. a) Tauc plot of In_2Se_3, CSZ-5-InSe, and CSZ-5-InBiSe derived from UV/Vis DRS. b) Mott–Schottky plots of CSZ-5-InSe and CSZ-5-InBiSe measured at a frequency of 1000 HZ. c) Schematic band structures of In_2Se_3, CSZ-5-InSe, and CSZ-5-InBiSe. d) The photocurrent–vlotage behavior for In_2Se_3, CSZ-5-InSe, and CSZ-5-InBiSe films; the inset shows the photoresponse under pulsed illumination at a constant potential of 0.6 V (vs. Ag/AgCl).

being larger than commercialized α-In_2Se_3 ($E_{BG} \approx 1.4$ eV) with condensed phase, lie well in the energy range suitable for photocatalytic applications in the visible-light region. The positive slope of the linear region on the MS plot measured at frequency of 1000 Hz in a 0.5 M sodium sulfate solution confirms **CSZ-5s** to be a n-type semiconductors. As shown in Figure 2b, the flat band potentials (E_{fb}) of **CSZ-5-InSe** and **CSZ-5-InBiSe** are approximately −0.55 and −0.41 V (vs. NHE), respectively. It is generally accepted that the flat band

potential of a n-type semiconductor equals its Fermi level and the conduction band edge of such n-type semiconductor is more negative by about 0.10 V than E_{fb}.[11] In this way, the conduction band of **CSZ-5-InSe** and **CSZ-5-InBiSe** can be approximately estimated to be −0.65 and −0.51 V (vs. NHE), respectively. In combination with the measured E_{BG} from DRS, we hence calculated their valence band potential at 1.45 V and 1.52 V, respectively. For comparison, the band position of commercialized In_2Se_3 was also determined (Figure S11). On the basis of the relationship between the normal electrode potential and the absolute vacuum energy with the numerical difference of 4.44,[12] the band position versus vacuum level could be also calculated (all above dada are well organized in Figure 2c and Table S5). Open-framework **CSZ-5-InSe** exhibits a slight lower E_{CB} and much lower E_{VB} comparing to condensed-phase In_2Se_3, however, the bismuth-doped **CSZ-5-InBiSe** has slight difference in its band position relative to original material of **CSZ-5-InSe**.

In order to investigate the effect of precise doping at specific sites on photo-electrochemical properties of resulting semiconductor zeolite framework, measurements on the potential-dependent photocurrent response were performed. As shown in Figure 2d, the anodic (positive) photocurrent responses indicate that **CSZ-5** exhibits n-type semiconductor characteristics under visible light illumination, which is consistent with the results obtained by Mott–Schottky measurements. The photocurrent traces of **CSZ-5/ITO** photoelectrodes show a rapid response and good reproducibility at the start and end of illumination. By applying biased potential of 0.6 V, the photoelectrodes of CSZ-5s can generate approximate photocurrent density from 0.20 (**CSZ-5-InSe**) to 0.50 μA cm^{-2} (**CSZ-5-InBiSe**) compared with the commercialized In_2Se_3 (0.30 μA cm^{-2}).

The **CSZ-5-InSe** materials have shown high electrocatalytic activity for the ORR, which is of the very essence to renewable energy technologies. More importantly, the electrocatalytic experiments reveal that the interrupted specific indium site X plays a crucial role in the oxygen reduction process. Although selenides with noble-metal ions (such as Ru, Ir) were widely studied as electrocatalysts in the ORR,[13] indium selenides have never been investigated as noble-metal-free electrocatalysts for the ORR. The cyclic voltammograms (CVs) of the ORR on **In_2Se_3/CB**(carbon black)-modified and **CSZ-5-InSe/CB-**modified glassy carbon (GC) electrodes are shown in Figure 3a. The **In_2Se_3/CB** electrode exhibited a poor ORR catalytic activity with the current density of the reduction peak and the potential at around 0.59 mA cm^{-2} and −0.32 V, respectively. Compared to In_2Se_3/CB, **CSZ-5-InSe/CB** had a much higher current density of the reduction peak at 1.56 mA cm^{-2} and a slight higher potential at around −0.29 V, indicating better catalytic performance. However, bismuth doping at specific sites deteriorated the catalytic activity of the original framework with a current density of 0.79 mA cm^{-2} at around −0.28 V. Rotating disk electrode (RDE) voltammetry was further performed to study the kinetics of the electrochemical catalytic ORR for **CSZ-5-InSe/CB**. Figure 3b showed that the current density was enhanced by increasing the rotating rate. The corresponding Koutecky–Levich (K–L) plots (the inset in Figure 3b, Table S6) demonstrated good linearity with parallelism over the potential range from −0.45 to −0.65 V, suggesting a similar electron-transfer number per O_2 molecule involved and first-order dependence of O_2 kinetics in the ORR. The electron transfer number of **CSZ-5-InSe/CB** was about 2.2, indicating that the **CSZ-5-InSe/CB** was close to the classical two-electron process. To further investigate whether the enhanced ORR activity originates mainly from specific sites or only from the porous structure of **CSZ-5-InSe**, another open framework material of UCR-2-InSe which possesses a similar composition and optical gap but no interrupted In sites was applied as electrocatalyst for the ORR (Figure S12 and Table S7).[14] Its electrocatalytic ORR behavior is very similar to that of In_2Se_3 and **CSZ-5-InSe**, however, shows a much lower current density. Therefore, although the detailed mechanism for the electrocatalytic ORR occurring at In–Se compounds still remains unclear, all the current results suggest that the indium ions on interrupted sites within the open-framework semiconductor material are responsible for the high activity, and thus are very likely the catalytic active sites.

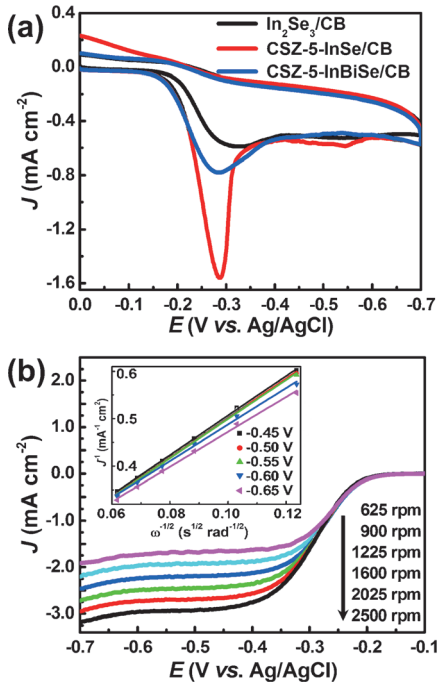

Figure 3. a) Cyclic voltammograms of In_2Se_3/CB, CSZ-5-InSe/CB, and CSZ-5-InBiSe/CB in O_2-saturated 0.1 M KOH solutions. Scan rate: 50 mV s^{-1}. b) RDE voltammograms at different rotation rates of CSZ-5-InSe/CB. Inset: the corresponding Koutecky–Levich plots at different potentials of CSZ-5-InSe/CB.

In conclusion, an interrupted chalcogenide-based semiconductor zeolite material has been created for the first time, and its band structure was also established by DRS and MS measurements. This n-type semiconductor material features a zeolitic framework with an entirely new boracite-related topology and interrupted metal sites. In particular, these specific indium sites serve as electrocatalytically active center in the ORR, and could be precisely doped by pyramidal three-coordinated trivalent Bi^{3+} ions with absolutely no Bi

present on other indium sites. **CSZ-5-InSe** displays superior electrocatalytic activity for the ORR compared to commercialized In_2Se_3 and bismuth-doped **CSZ-5-InBiSe**. The atomically precise doping implemented at the zeolitic semiconductor material with specifically interrupted sites represents a promising new strategy for the fine regulation of the electronic structure and the photoelectrical properties of the semiconductor materials. Our study reveals deliberate doping at the interrupted sites, which could be a facile route to property engineering for CSZ materials or even oxide-based zeolites with interrupted sites. Atomic precise doping with other metal ions and a more detailed electrocatalytic mechanism of In–Se-involved ORR is still under investigation.

Keywords: electrochemistry · interrupt structures · mesoporous materials · oxygen reduction reaction · zeolite-analog semiconductors

How to cite: *Angew. Chem. Int. Ed.* **2015**, *54*, 5103–5107
Angew. Chem. **2015**, *127*, 5192–5196

[1] a) Y. Li, J. H. Yu, *Chem. Rev.* **2014**, *114*, 7268–7316; b) M. Milina, S. Mitchell, D. Cooke, P. Crivelli, J. Pérez-Ramírez, *Angew. Chem. Int. Ed.* **2015**, *54*, 1591–1594; *Angew. Chem.* **2015**, *127*, 1611–1614; c) X. Li, Q. M. Sun, Y. Li, N. Wang, J. R. Lu, J. H. Yu, *J. Phys. Chem. C* **2014**, *118*, 24935–24940; d) F. J. Liu, T. Willhammar, L. Wang, L. F. Zhu, Q. Sun, X. J. Meng, W. Carrillo-Cabrera, X. D. Zou, F. S. Xiao, *J. Am. Chem. Soc.* **2012**, *134*, 4557–4560; e) D. Xie, L. B. McCusker, C. Baerlocher, S. I. Zones, W. Wan, X. D. Zou, *J. Am. Chem. Soc.* **2013**, *135*, 10519–10524; f) G. J. Yang, Y. X. Wei, S. T. Xu, J. R. Chen, J. Z. Li, Z. M. Liu, J. H. Yu, R. R. Xu, *J. Phys. Chem. C* **2013**, *117*, 8214–8222.

[2] C. Baerlocher, L. B. McCusker, *Database of Zeolite Structures*, http://www.iza-structure.org/databases/.

[3] a) W. Hua, H. Chen, Z. B. Yu, X. D. Zou, J. H. Lin, J. L. Sun, *Angew. Chem. Int. Ed.* **2014**, *53*, 5868–5871; *Angew. Chem.* **2014**, *126*, 5978–5981; b) J. L. Sun, C. Bonneau, Á. Cantín, A. Corma, M. J. Díaz-Cabañas, M. Moliner, D. L. Zhang, M. R. Li, X. D. Zou, *Nature* **2009**, *458*, 1154–1157; c) J. X. Jiang, J. L. Jorda, J. H. Yu, L. A. Baumes, E. Mugnaioli, M. J. Díaz-Cabañas, U. Kolb, A. Corma, *Science* **2011**, *333*, 1131–1134; d) T. Willhammar, J. L. Sun, W. Wan, P. Oleynikov, D. L. Zhang, X. D. Zou, M. Moliner, J. Gonzalez, C. Martínez, F. Rey, A. Corma, *Nat. Chem.* **2012**, *4*, 188–194; e) T. Willhammar, A. W. Burton, Y. F. Yun, J. L. Sun, M. Afeworki, K. G. Strohmaier, H. Vroman, X. D. Zou, *J. Am. Chem. Soc.* **2014**, *136*, 13570–13573; f) Y. Wei, Z. J. Tian, H. Gies, R. S. Xu, H. Ma, R. Y. Pei, W. P. Zhang, Y. P. Xu, L. Wang, K. D. Li, B. C. Wang, G. D. Wen, L. W. Lin, *Angew. Chem. Int. Ed.* **2010**, *49*, 5367–5370; *Angew. Chem.* **2010**, *122*, 5495–5498; g) S. Smeets, D. Xie, C. Baerlocher, L. B. McCusker, W. Wan, X. D. Zou, S. I. Zones, *Angew. Chem. Int. Ed.* **2014**, *53*, 10398–10402; *Angew. Chem.* **2014**, *126*, 10566–10570; h) J. X. Jiang, Y. F. Yun, X. D. Zou, J. L. Jorda, A. Corma, *Chem. Sci.* **2015**, *6*, 480–485.

[4] N. F. Zheng, X. H. Bu, B. Wang, P. Y. Feng, *Science* **2002**, *298*, 2366–2369.

[5] a) C. Wang, X. H. Bu, N. F. Zheng, P. Y. Feng, *Chem. Commun.* **2002**, 1344–1345; b) P. Vaqueiro, *Inorg. Chem.* **2008**, *47*, 20–22; c) M. J. Manos, C. D. Malliakas, M. G. Kanatzidis, *Chem. Eur. J.* **2007**, *13*, 51–58; d) W. W. Xiong, E. U. Athresh, Y. T. Ng, J. F. Ding, T. Wu, Q. C. Zhang, *J. Am. Chem. Soc.* **2013**, *135*, 1256–1259; e) H. Li, A. Laine, M. O'Keeffe, O. M. Yaghi, *Science* **1999**, *283*, 1145–1147; f) Q. C. Zhang, Y. Liu, X. H. Bu, T. Wu, P. Y. Feng, *Angew. Chem. Int. Ed.* **2008**, *47*, 113–116; *Angew. Chem.* **2008**, *120*, 119–122; g) Q. C. Zhang, X. H. Bu, J. Zhang, T. Wu, P. Y. Feng, *J. Am. Chem. Soc.* **2007**, *129*, 8412–8413; h) X. H. Bu, N. F. Zheng, Y. Q. Li, P. Y. Feng, *J. Am. Chem. Soc.* **2002**, *124*, 12646–12647; i) C. Wang, X. H. Bu, N. F. Zheng, P. Y. Feng, *J. Am. Chem. Soc.* **2002**, *124*, 10268–10269; j) Y. M. Lin, W. Massa, S. Dehnen, *Chem. Eur. J.* **2012**, *18*, 13427–13434; k) Y. M. Lin, S. Dehnen, *Inorg. Chem.* **2011**, *50*, 7913–7915; l) J. Lin, Q. Zhang, L. Wang, X. C. Liu, W. B. Yan, T. Wu, X. Bu, P. Feng, *J. Am. Chem. Soc.* **2014**, *136*, 4769–4779; m) T. Wu, Q. Zhang, Y. Hou, L. Wang, C. Mao, S. Zheng, X. Bu, P. Feng, *J. Am. Chem. Soc.* **2013**, *135*, 10250–10253.

[6] a) J. X. Jiang, J. L. Jorda, M. J. Díaz-Cabañas, J. H. Yu, A. Corma, *Angew. Chem. Int. Ed.* **2010**, *49*, 4986–4988; *Angew. Chem.* **2010**, *122*, 5106–5108; b) F. J. Chen, Y. Xu, H. B. Du, *Angew. Chem. Int. Ed.* **2014**, *53*, 9592–9596; *Angew. Chem.* **2014**, *126*, 9746–9750; c) M. Estermann, L. B. McCusker, C. Baerlocher, A. Merrouche, H. Kessler, *Nature* **1991**, *352*, 320–323; d) J. X. Jiang, J. H. Yu, A. Corma, *Angew. Chem. Int. Ed.* **2010**, *49*, 3120–3145; *Angew. Chem.* **2010**, *122*, 3186–3212; e) G. Y. Yang, S. C. Sevov, *J. Am. Chem. Soc.* **1999**, *121*, 8389–8390; f) G. Z. Liu, S. T. Zheng, G. Y. Yang, *Angew. Chem. Int. Ed.* **2007**, *46*, 2827–2830; *Angew. Chem.* **2007**, *119*, 2885–2888; g) J. X. Jiang, Y. Xu, P. Cheng, Q. M. Sun, J. H. Yu, A. Corma, R. R. Xu, *Chem. Mater.* **2011**, *23*, 4709–4715.

[7] B. Wang, A. P. Cote, H. Furukawa, M. O'Keeffe, O. M. Yaghi, *Nature* **2008**, *453*, 207–211.

[8] H. X. Zhang, F. Wang, H. Yang, Y. X. Tan, J. Zhang, X. Bu, *J. Am. Chem. Soc.* **2011**, *133*, 11884–11887.

[9] a) Y. Han, Y. Li, J. Yu, R. Xu, *Angew. Chem. Int. Ed.* **2011**, *50*, 3003–3005; *Angew. Chem.* **2011**, *123*, 3059–3061; b) Y. Xu, Y. Li, Y. Han, X. Song, J. Yu, *Angew. Chem. Int. Ed.* **2013**, *52*, 5501–5503; *Angew. Chem.* **2013**, *125*, 5611–5613.

[10] V. B. Nascimento, V. E. de Carvalho, R. Paniago, E. A. Soares, L. O. Ladeira, H. D. Pfannes, *J. Electron Spectrosc. Relat. Phenom.* **1999**, *104*, 99–107.

[11] S. Saha, G. Das, J. Thote, R. Banerjee, *J. Am. Chem. Soc.* **2014**, *136*, 14845–14851.

[12] W. J. Chun, A. Ishikawa, H. Fujisawa, T. Takata, J. N. Kondo, M. Hara, M. Kawai, Y. Matsumoto, K. Domen, *J. Phys. Chem. B* **2003**, *107*, 1798–1803.

[13] a) I. V. Malakhov, S. G. Nikitenko, E. R. Savinova, D. I. Kochubey, N. Alonso-Vante, *J. Phys. Chem. B* **2002**, *106*, 1670–1676; b) A. Lewera, J. Inukai, W. P. Zhou, D. Cao, H. T. Duong, N. Alonso-Vante, A. Wieckowski, *Electrochim. Acta* **2007**, *52*, 5759–5765; c) G. Liu, H. Zhang, *J. Phys. Chem. C* **2008**, *112*, 2058–2065.

[14] C. Wang, X. Bu, N. F. Zheng, P. Feng, *Angew. Chem. Int. Ed.* **2002**, *41*, 1959–1961; *Angew. Chem.* **2002**, *114*, 2039–2041.

Received: January 23, 2015
Published online: February 26, 2015

